Projection-Based Model Order Reduction for Steady Aerodynamics

Alexander Vendl and Heike Faßbender

TU Braunschweig, Institute *Computational Mathematics*, AG Numerik, Fallersleber-Tor-Wall 23, 38106 Braunschweig, Germany.

Abstract. Nonlinear model order reduction techniques for systems often make use of Proper Orthogonal Decomposition (POD). In this work a method based on POD, called Missing Point Estimation (MPE), is investigated. It is capable of efficiently simulating steady-state flows with the angle of attack as a system parameter. The basic idea of MPE is to project the governing equations onto the POD subspace in such a way that the resulting reduced order model does not have to evaluate the right hand side at each and every grid point, but a few selected points. While the projection onto the POD subspace yields a reduced order model, the limitation to only few points actually achieves independence from the full order of the governing equations. To demonstrate the effectiveness of this method, numerical results for the simulation of inviscid, steady-state flows past a three-dimensional, complex airplane configuration are given.

Keywords: Model Order Reduction, Missing Point Estimation, Proper Orthogonal Decomposition, CFD, Steady Aerodynamics

1 Introduction

The European aviation industry is facing great challenges: Their products have to be more fuel-efficient, safer, and the European industry has to to remain competitive with traditional competitors from the US and upcoming ones, e.g. from China [1].

In order to tackle these challenges, numerical simulations play an essential role. In fact, due to the steadily increasing computational power, numerical simulations become more and more effective. Today's vision is that *digital flight-tests* [2–4] are possible in the future, that is, supporting current testing methods such as wind tunnel experiments and flight testing by numerical simulations.

For this vision to become true, however, numerical methods need to be less time-consuming. To achieve this, either new high performance computing methods have to be developed in order to be able to simulate the constantly ameliorated mathematical models or (new) model reduction techniques have to be employed in order to attain adaquate simplified models which allow fast simulation. This work is concerned with the latter.

The goal of model order reduction is to significantly reduce the number of equations to be solved and thereby decreasing the time spend on solving the

system. Note that the number of equations of a system is also referred to as the order. Often the solution trajectories of high-fidelity models of order N lie in low dimensional subspaces of order k ¡¡ N. Making use of this fact, one can construct a projection with which the full-order system is reduced to one of smaller order.

In context of Computational Fluid Dynamics such a low-dimensional subspace, in which the solution trajectory resides, can be created with the help of Proper Orthogonal Decomposition (POD). POD uses so-called snapshots, which are solutions of the system, and stores these in a matrix, called the snapshot matrix. Subsequently, the Singular Value Decomposition of this matrix is computed. This yields the left singular vectors, which are an orthogonal basis for a subspace, in which the snapshots lie. It is assumed that if the snapshots are characteristic for the solutions, which are to be computed by the reduced order model, then the latter also lie in this subspace.

While for linear systems the projection of the equations suffices to dramatically speed up the simulation, this is usually not the case for nonlinear systems. Note that for nonlinear systems the projected nonlinear right hand side is of lower order, but in order to evaluate it, one usually needs to evalute the original full-order right-hand side. As a result, there is still a dependence on the full order and, thus, a significant speed-up cannot be expected. In recent years, model order reduction techniques have been developed, which address this issue by constructing projections that do not need to evaluate the full order right hand side as a whole. Rather, only some components of the right hand side have to be computed. Among these methods are the Discrete Empirical Interpolation Method (DEIM) [5] and the Missing Point Estimation (MPE) [6].

The latter approach is pursued in this work. It has been introduced in [7] and has since been applied to various fields of application, among which are heat transfer processes [6], electrical circuit modeling [8], and oil reservoir simulation [9]. The authors are unaware of any applications of MPE to aerodynamic flow problems, other than their own [10, 11].

There are, of course, other projection-based model order reduction reduction techniques in aerodynamics: One very similar to MPE, in the way that the reduced order modeling is carried out on the discrete equations, is the subspace projection method [12]. Unlike the MPE, it evaluates the full order residual. Despite the dependence on the full order, a speed-up is achieved due to the fact that a larger time step can be chosen in the reduced order model compared to the full order model.

Secondly, the so-called Galerkin Projection method has been used in many publications on reduced order models in aerodynamics. This method carries out the reduced order modeling on the continuous equations [13, 14].

Finally, there is an approach, called the Least-squares ROM method, which is not based on projection [15–19]. It has been introduced in context of steady aerodynamics [15], for which the right hand side – or residual – becomes zero. It minimizes the residual in a least-squares sense in the POD subspace.

The work is organized as follows. After this introduction, the full order governing equations and its notations are presented in the next section. Then in

Section 3 the Proper Orthogonal Decomposition is described, which is the foundation for the Missing Point Estimation considered in this work. The Missing Point Estimation is outlined in Section 4. After presenting numerical results for a three-dimensional flow past an airplane configuration in Section 5, conclusions to this work are given in the last section.

2 The full order governing equations

The flow problem, which is considered in this work, is modeled by the Euler equations. The Euler equations are given by

$$\int_{\Omega} \frac{\partial \boldsymbol{W}}{\partial t} \, \mathrm{d}\Omega + \oint_{S} \boldsymbol{F} \cdot \, \mathrm{d}S = 0 \; , \tag{1}$$

where

$$\boldsymbol{W}^T = \left(\rho, \, \rho \, v_x, \, \rho \, v_y, \, \rho \, v_z, \, \rho \, E \right) \tag{2}$$

is the vector of the conservative variables, which are the density ρ, the Cartesian velocity components v_x, v_y, v_z, and the total energy E. The flux vector $\boldsymbol{F}$ contains the convective flux through the boundaries $S = \partial\Omega$ of the control volumes Ω [20, chapter 2].

When the control volume Ω in (1) is spatially discretized with a finite-volume approach [20] for a computational grid of N grid cells, a set of ordinary differential equations of the form

$$\frac{\mathrm{d}\boldsymbol{w}(t;\alpha)}{\mathrm{d}t} = -\tilde{V}^{-1} \boldsymbol{R}(\boldsymbol{w}(t;\alpha)) \tag{3}$$

is obtained, where α is the angle of attack and a parameter to the system. In the above equation

$$\boldsymbol{w}^T = \left(\; \boldsymbol{\rho}^T, \; \boldsymbol{\rho v_x}^T, \; \boldsymbol{\rho v_y}^T, \; \boldsymbol{\rho v_z}^T, \; \boldsymbol{\rho E}^T \; \right) \in \mathbb{R}^{5N} \; , \tag{4}$$

is the the discrete vector of conservative variables. Each of the entries $\boldsymbol{\rho}$, $\boldsymbol{\rho v_x}$, $\boldsymbol{\rho v_y}$, $\boldsymbol{\rho v_z}$, and $\boldsymbol{\rho E}$ is a discretization of the corresponding conservative variable and is stored in a vector of size N. The residual vector $\boldsymbol{R} \in \mathbb{R}^{5N}$ is ordered accordingly and is the discretization of the flux integral in (1). Furthermore, $\tilde{V} = \mathrm{diag}(V, \ldots, V) \in \mathbb{R}^{5N \times 5N}$ is a block diagonal matrix, where each block is given by the diagonal matrix $V \in \mathbb{R}^{N \times N}$, whose entries are the volumes of the respective grid cell.

Note that in case steady flows are considered the time derivative drops and (3) simplifies to

$$\boldsymbol{0} = -\tilde{V}^{-1} \boldsymbol{R}(\boldsymbol{w}(t;\alpha)) \; . \tag{5}$$

3 Proper Orthogonal Decomposition

In this section a short review of Proper Orthogonal Decomposition is given. A more comprehensive introduction can be found in [21].

Let $\boldsymbol{w}_1, \ldots, \boldsymbol{w}_m$ be steady CFD flow solutions of (3), called snapshots, for different flow conditions, e.g. $\boldsymbol{w}_i = \boldsymbol{w}(\alpha_i)$, where α_i the angle of attack for the particular flow. With these snapshots the corresponding centered snapshot matrix is given by

$$Y = (\bar{\boldsymbol{w}}_1, \ldots, \bar{\boldsymbol{w}}_m) \ , \tag{6}$$

where $\bar{\boldsymbol{w}}_i = \boldsymbol{w}_i - \bar{\boldsymbol{w}}$ are the centered snapshots around the mean flow $\bar{\boldsymbol{w}} = \frac{1}{m}\sum_{i=1}^{m} \boldsymbol{w}_i$.

Consider the L_2 scalar product $(\boldsymbol{w}_i, \boldsymbol{w}_j)_{L_2} = \boldsymbol{w}_i^T \tilde{V} \boldsymbol{w}_j$. The goal of POD is to find an orthonormal basis U which spans the space of the snapshots, i.e. $\operatorname{span} U = \operatorname{span} Y$. This basis can be obtained by first solving the symmetric eigenvalue problem

$$Y^T \tilde{V} Y \boldsymbol{\psi}_j = \lambda_j \boldsymbol{\psi}_j \ , \tag{7}$$

where the eigenvectors ψ_j are normalized, that is, $\boldsymbol{\psi}_j^T \boldsymbol{\psi}_j = 1$, and, subsequently, computing

$$\boldsymbol{u}_j = \frac{1}{\sqrt{\lambda_j}} Y \boldsymbol{\psi}_j \ . \tag{8}$$

Note that the basis is in fact orthonormal in sense of the L_2 scalar product, since

$$(\boldsymbol{u}_i^T, \boldsymbol{u}_j)_{L_2} = \frac{1}{\sqrt{\lambda_i \lambda_j}} \boldsymbol{\psi}_i^T Y^T \tilde{V} Y \boldsymbol{\psi}_j = \frac{\lambda_j}{\sqrt{\lambda_i \lambda_j}} \boldsymbol{\psi}_i^T \boldsymbol{\psi}_j = \delta_{ij} \tag{9}$$

and $\boldsymbol{\psi}_i^T \boldsymbol{\psi}_j = \delta_{ij}$ due to the fact that the eigenvalue problem (7) is symmetric.

Take note of the fact that the columns of the centered snapshot matrix are linearly dependent. In fact, the sum of all columns is zero. Hence, the smallest eigenvalue is exactly zero.

Assume that the eigenvectors $\boldsymbol{\psi}_i$ are ordered according to the magnitude of their corresponding eigenvalues, i.e. $\lambda_1 \geq \lambda_2 \geq \ldots \geq \lambda_m$. Then the basis $U = (\boldsymbol{u}_1, \ldots, \boldsymbol{u}_m)$ can be truncated to contain only the most relevant modes. In this work the relative information content [22] is used, which is defined as

$$RIC(d) = \frac{\sum_{i=1}^{d} \lambda_i}{\sum_{j=1}^{m} \lambda_j} \ . \tag{10}$$

The dimension d is then chosen such that the relative information content is larger than a prescribed percentage δ, i.e. $RIC(d) \geq \delta$. Note that the space spanned by the first $d \leq m$ basis modes is the best representation of dimension d of the space spanned by the snapshots.

Flow solutions in this space can then be represented by

$$\boldsymbol{w} = U_d \boldsymbol{a} + \bar{\boldsymbol{w}} \ , \tag{11}$$

where $U_d = (\boldsymbol{u}_1, \ldots, \boldsymbol{u}_d)$ is the (truncated) POD basis and $\boldsymbol{a} = (a_1, \ldots, a_d)$ the vector of the corresponding coefficients. All reduced order models employing POD boil down to determining this vector $\boldsymbol{a}$ of POD coefficients in different ways.

4 Missing Point Estimation

In this work a projection-based method called Missing Point Estimation (MPE) is used to obtain the reduced order model (ROM). It has been introduced in [7]. While the most prominent projection-based method, called Galerkin projection, projects all equations onto the POD subspace, the Missing Point Estimation does so only for some selected equations. This has the advantage that the reduced order model is much more efficient.

Before the MPE is reviewed in detail, we want to give a motivation why considering only some equations is beneficial: The Galerkin projection of the governing equations (3) is given by

$$\frac{\mathrm{d}\boldsymbol{a}(t;\alpha)}{\mathrm{d}t} = -U_d^T \boldsymbol{R}(U_d \boldsymbol{a}(t;\alpha) + \bar{\boldsymbol{w}}) \ , \tag{12}$$

Note that system is of the order of the POD subspace, i.e. d, since the system only depends on the coefficient vector $\boldsymbol{a}(t;\alpha) \in \mathbb{R}^d$. However, in order to solve the system, in each time step the residual vector $\boldsymbol{R} \in \mathbb{R}^5 N$ has to be computed, which is of the order $5N$ of the original system. As a result, no significant speed-up for a single time step can be expected.

In the following MPE is reviewed in the context of the Euler equations. For a detailed account of the method the reader is referred to [6]. Consider the spatially discretized governing equations

$$\frac{\mathrm{d}\boldsymbol{w}(t;\alpha)}{\mathrm{d}t} = -\tilde{V}^{-1} \boldsymbol{R}(\boldsymbol{w}(t;\alpha)) \ , \tag{13}$$

where α is the angle of attack and the only varying parameter in the model. If the POD representation of the flow is inserted into this set of equations, i.e.

$$\frac{\mathrm{d}U_d\boldsymbol{a}(t;\alpha)}{\mathrm{d}t} = -\tilde{V}^{-1} \boldsymbol{R}(U_d \boldsymbol{a}(t;\alpha) + \bar{\boldsymbol{w}}) + \boldsymbol{\epsilon}_0 \ , \tag{14}$$

an error ϵ_0 is introduced. Note that $\frac{\mathrm{d}\bar{\boldsymbol{w}}}{\mathrm{d}t} = 0$, since the mean flow is independent of time.

In oder to construct a more efficient reduced order model, the MPE neglects some function evaluations in the right-hand side vector R. It is assumed that the information missed in this way is well captured by the information used due to the spatial correlation in the POD basis. Since each equation of the spatially discretized system corresponds to a grid point, the missing – or not considered – points are estimated. This gives the Missing Point Estimation its name.

In order to formulate the negligence of equations mathematically, a filtering or selection matrix is defined. Let us assume that the selected equations correspond to the indices of the grid points, which are given by $\mathbb{X} = \{j_1, \ldots, j_n\} \subset \{1, \ldots, N\}$, where N is the total number of grid points and n is the number of the selected points. Then the filtering matrix is defined as

$$P = \left(\boldsymbol{e}_{j_1} \cdots \boldsymbol{e}_{j_n} \right) \in \mathbb{R}^{N \times n} \tag{15}$$

with the help of the unit vectors $e_j \in \mathbb{R}^N$. Note that this filtering matrix is only applicable to one flow variable. In order to construct one for all variables, P appears for each variable as a diagonal block, i.e. $\tilde{P} = \mathrm{diag}(P, \ldots, P) \in \mathbb{R}^{5N \times 5n}$. Note that the matrix $\mathit{\Pi}_{\tilde{P}} = \tilde{P}\tilde{P}^T \in \mathbb{R}^{5N \times 5N}$ is a diagonal matrix, which is a projection onto the equations corresponding to the selected points. Applying $\mathit{\Pi}_{\tilde{P}}$ to (14) yields

$$\tilde{P}\tilde{P}^T U_d \frac{\mathrm{d}\boldsymbol{a}(t;\alpha)}{\mathrm{d}t} = -\tilde{P}\tilde{P}^T \tilde{V}^{-1} \boldsymbol{R}(U_d \boldsymbol{a}(t;\alpha) + \bar{\boldsymbol{w}}) + \tilde{P}\tilde{P}^T \boldsymbol{\epsilon}_0 \ . \tag{16}$$

Next, orthogonality conditions are imposed upon the system. They require the error at the selected points to be orthogonal to the POD subspace, i.e. $\left(\boldsymbol{u}_j, \tilde{P}\tilde{P}^T \boldsymbol{\epsilon}_0 \right)_{L_2} = \boldsymbol{0}$ for $j = 1, \ldots, d$. It follows that

$$U_d^T \tilde{V} \tilde{P}\tilde{P}^T U_d \frac{\mathrm{d}\boldsymbol{a}(t;\alpha)}{\mathrm{d}t} = -U_d^T \tilde{V} \tilde{P}\tilde{P}^T \tilde{V}^{-1} \boldsymbol{R}(U_d \boldsymbol{a}(t;\alpha) + \bar{\boldsymbol{w}}) \ . \tag{17}$$

Elimination of the matrix $U_d^T \tilde{V} \tilde{P}\tilde{P}^T U_d$ by premultiplying with its inverse, finally yields the MPE reduced order system

$$\frac{\mathrm{d}\boldsymbol{a}(t;\alpha)}{\mathrm{d}t} = -\left(U_d^T \tilde{V} \tilde{P}\tilde{P}^T U_d \right)^{-1} U_d^T \tilde{P}\tilde{P}^T \boldsymbol{R}(U_d \boldsymbol{a}(t;\alpha) + \bar{\boldsymbol{w}}) \ . \tag{18}$$

It is of reduced complexity, since its order is $d \ll 5N$. In addition, due to fact that the residual vector $\boldsymbol{R}$ is premultiplied with the filtering matrix $\tilde{P}^T$, it does not have to be evaluated at each and every point, but only at the few selected points.

For steady flows, as considered in this work, the time derivative drops, that is

$$\boldsymbol{0} = -\left(U_d^T \tilde{V} \tilde{P}\tilde{P}^T U_d \right)^{-1} U_d^T \tilde{P}\tilde{P}^T \boldsymbol{R}(U_d \boldsymbol{a}(\alpha) + \bar{\boldsymbol{w}}) \ . \tag{19}$$

As a result the above system can be solved with a Newton-type of method. In fact, Powell's Dog Leg method [23] is used. As an initial start vector for the POD coefficients the mean flow is chosen, that is, $\boldsymbol{a} = \boldsymbol{0}$.

5 Results

The investigated method of this work, the Missing Point Estimation, is tested on a complex three-dimensional aircraft configuration called DLR-F12. It is a

wing-body configuration with a vertical and horizontal stabilizer (see Fig. 1). The computational grid consists of about 670 thousand grid points ($N = 669,062$). It is shown in Fig. 1. All compuations are carried out with the CFD solver TAU [24]

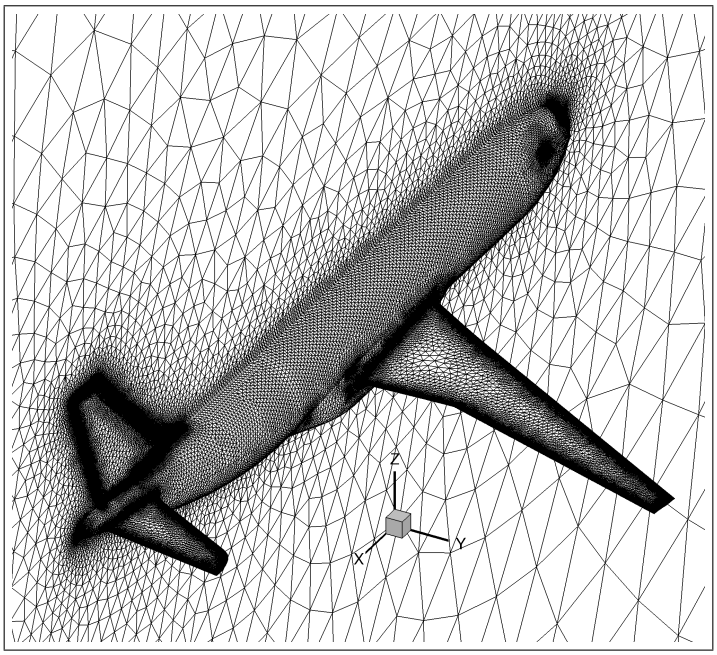

Fig. 1. The computational grid of the DLR F12 configuration.

The inviscid flow – modeled by the Euler equations – at a subsonic Mach number of $M_\infty = 0.2$ is computed. Euler equations are used in order to keep the number of grid points low enough such that the solutions are computable on a desktop computer. Note that Navier-Stokes simulations typically require much more grid points than the Euler equations. In order to set up the MPE reduced order model, snapshots are needed for the computation of the POD. Here, snapshots at different angles of attack at the Mach number $M_\infty = 0.2$ are taken. To be more precise, $\alpha \in \{0°, 2°, 4°, 6°, 8°\}$. The reduced order model (19) is then used to compute flows at intermediate angles. At first, consider $\alpha = 5°$.

In the snapshot computations, the residual is lowered by fourteen orders of magnitude by conducting ten thousand iterations. As initial solutions, freestream values are utilized.

In the following, different characteristics of the MPE reduced order model are looked at. These include the influence that the number of used modes as well as the selected points have on the accuracy of the approximate solution. Fur-

thermore, the computational time and the results for other intermediate angles of attack are investigated.

Influence of the number of used modes: At first, we take a look at the role that the number of modes, which are used in the MPE reduced order system, play on the quality of the approximation. In order to get an idea of the importance of each of the modes, we consider the relative energy content. It is given by

$$E(j) = \frac{\lambda_j}{\sum_{i=1}^{m} \lambda_i} \ , \tag{20}$$

where the λ_j are the eigenvalues of the symmetric eigenproblem (7).

Note that m is equal to number of snapshots, i.e $m = 5$. Table 1 reveals how much relative energy content each of the modes carries. Note that the fifth mode does not carry any energy. This is due to the fact that the columns of the centered snapshot matrix are linear dependent and as consequence the smallest eigenvalue is zero.

Table 1. Relative energy content of the modes corresponding to the snapshots at $\alpha \in \{0°, 2°, 4°, 6°, 8°\}$ of the DLR F12 configuration at $M_\infty = 0.2$.

j	1	2	3	4	5
$E(j)$	$9.99560 \cdot 10^{-1}$	$4.40291 \cdot 10^{-4}$	$1.81356 \cdot 10^{-7}$	$1.04662 \cdot 10^{-8}$	0

Note further that the first basis vector contains more than 99.9% and the first two together hold more than 99.9999% of the energy. This suggests that the first two modes (along with the mean flow $\bar{\boldsymbol{w}}$) suffice to reconstruct the snapshots and, presumably, also to obtain accurate solutions at intermediate angles of attack.

In order to substantiate this presumption, we investigate the quality of the approximation by the MPE system for the different choices of the number of modes. As an indicator for the approximation quality, we look at the lift and drag coefficients, i.e. c_l and c_d, respectively. Table 2 shows the results.

In order to eradicate any influence of the selection of points on the MPE reduced order model, we evaluate the residual at the same points in each computation. As a matter of fact, only the farfield points are considered, which is a good point selection, as we will later see.

Note that one mode does suffice to obtain an acceptable approximation. In fact, in this case the relative error in the drag coefficient is more than 25 %. When using two basis vectors, the drag coefficient is slightly overestimated by the MPE, while it is underestimated when employing three or four.

Influence of the selected points: In the following we want to investigate the influence that the selection of points has on the prediction of the aerodynamic

Table 2. Lift and drag coefficients of the DLR F12 configuration at $M_\infty = 0.2$ computed with MPE, where the residual evaluations are restricted to the farfield points. The aerodynamic coefficients are predicted at $\alpha = 5^\circ$ for different numbers of modes m and compared to the CFD reference solution at the same angle.

# of modes	residual evaluations	c_l (error in %)	c_d (error in %)
$d = 1$	8	$5.803 \cdot 10^{-1}$ (0.41%)	$1.449 \cdot 10^{-2}$ (26.82%)
$d = 2$	10	$5.827 \cdot 10^{-1}$ (0.0%)	$1.983 \cdot 10^{-2}$ (0.15%)
$d = 3$	14	$5.827 \cdot 10^{-1}$ (0.0%)	$1.975 \cdot 10^{-2}$ (0.25%)
$d = 4$	17	$5.827 \cdot 10^{-1}$ (0.0%)	$1.975 \cdot 10^{-2}$ (0.25%)
CFD	2000	$5.827 \cdot 10^{-1}$	$1.980 \cdot 10^{-2}$

coefficients for the proposed method. Since two modes yield better results when using the point selection of farfield points in MPE, both two and four modes are considered.

Besides the already considered point selection (only farfield boundary), we consider three other ones. All of them will include the farfield boundary due to the fact that there, the system's parameter, the angle of attack, is set. First of all, we select points, which are on and close to the surface. This is done by specifying a minimal and maximal distance from the surface. The specifics can be found in Table 3. With this selection a large part of the computational grid is chosen. In order to reduce the number of selected points, only those which are a bit further from the surface are chosen. Again, specifics can be found in Table 3. Last, but not least, all points are used, at which the equations are solved.

Table 3. The definition of the point selections for the DLR F12 configuration at $M_\infty = 0.2$, where min/max distance stands for the minimal and maximal distance from the surface of the configuration in spatial units (length of the airfoil = 1.0 units). Note that FF shall be an abbreviation for the farfield.

point selection	# of points	min distance	max distance
I (entire farfield)	336	-	-
II (FF + points close to surface)	633281	0.0	0.05
III (FF + points further from surface)	16279	0.05	0.1
IV (all points)	669062	0.0	100.0

For all these point selections the aerodynamic coefficients are predicted with the help of MPE using two as well as four modes. Table 4 shows the results. Note that if two modes are employed, all point selections yield the same lift and drag coefficient, except in case all points are considered. In this latter case the drag coefficient is slightly worse. Note further that when using four modes the MPE method is not as robust as when using two modes with respect to the

point selections. In fact, with selections II and IV there is no convergence at all. In these computations the first iteration of the Dog Leg method yields an unphysical flow. As a result the residual can not be computed.

Table 4. Lift and drag coefficients computed with MPE for different point selections for the DLR-F12 configuration at $M_\infty = 0.2$ and $\alpha = 5^\circ$.

point selection	# modes	residual eval's	c_l (error in %)	c_d (error in %)
I, II, III	d=2	10	$5.827 \cdot 10^{-1}$ (0.0%)	$1.983 \cdot 10^{-2}$ (0.15%)
IV	d=2	10	$5.827 \cdot 10^{-1}$ (0.0%)	$1.984 \cdot 10^{-2}$ (0.20%)
I	d=4	17	$5.827 \cdot 10^{-1}$ (0.0%)	$1.975 \cdot 10^{-2}$ (0.25%)
II, IV	d=4	-	-	-
III	d=4	17	$5.827 \cdot 10^{-1}$ (0.0%)	$1.976 \cdot 10^{-2}$ (0.20%)
CFD	-	2000	$5.827 \cdot 10^{-1}$	$1.980 \cdot 10^{-2}$

All in all, using two modes and only the farfield points (selection I) is the most effective point selection. Not only does it yield the best result for the drag coefficient with respect to all considered tests, but it also contains the least number of points. This means that only few equations need to be solved. In addition, the farfield points can easily be identified. Figure 2 shows the pressure distribution on the surface of the DLR-F12 configuration both for the CFD reference solution as well as the MPE solution using only the farfield points. Both solutions are hardly distinguishable, which of course means, that the MPE approximates the CFD reference well.

Computational time: After having looked at important characteristics, which influence the quality of the approximation, we now examine the computational time. Table 5 reveals both the time needed for computing the MPE as well as the CFD solution. Both computations are carried out for ten consecutive runs and then the average is given. Note that the CFD computation is started from freestream values and the residual is decreased by seven orders of magnitude after conducting two thousand iterations.

Note that the computation of the reduced order solution is obtained more than one hundred times faster than the CFD solution. This is mainly due to the fact that only ten, rather than two thousand residual evaluations are needed. Note that the MPE has not been implemented efficiently yet. In fact the residual is evaluated at each and every point and is then filtered according to the point selection. An implementation, which evaluates the residual only at the relevant points, would of course be more efficient. It is, however, technically challenging and needs an intrusion into the CFD solver Tau. Note that only 17.102 seconds of the overall computational time for MPE are spend on reading the snapshots and computing the POD. Consequently, it is expected that an efficient implementation has a lot of room for improvement.

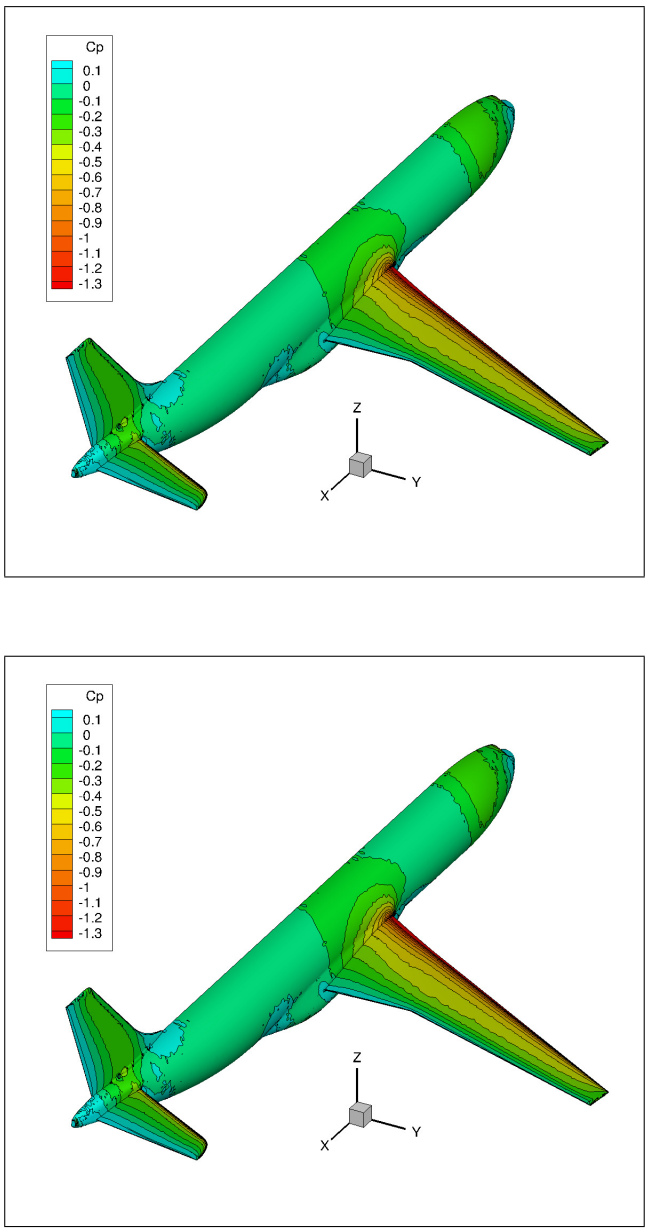

Fig. 2. The pressure distribution on the surface of the DLR F12 configuration $M_\infty = 0.2$ and $\alpha = 5^\circ$ for the CFD reference solution (top) and the MPE (bottom) computed using only the farfield points and $d = 2$ modes.

Table 5. Computational time for the DLR F12 configuration at $M_\infty = 0.2$ computed with the MPE using only the farfield points and $d = 2$ modes as well as with CFD. The time for MPE includes the computation of POD, but not the generation of the snapshots. Since MPE is not efficiently implemented yet, the time is expected to be less. Hence the $<$ sign.

model	residual evaluations	time (in CPU s)
MPE (farfield points)	10	< 117.743
CFD	2000	15103.1

As a matter of fact, assuming that the evaluation of the residual requires the same amount of time at each point and that most of the time for solving the system ($T = 117.743 - 17.102 = 100.641$ CPU s) is spent on evaluating the residual, a very rough estimate of the time for an efficient implementation would be $T * n/N$. This leads to 0.051 CPU s when using only the farfield points for MPE. But even if the time is much higher than this rough estimate, it is obviously the time spend on reading the snapshots and computing POD that dominates.

Solutions at other angles of attack: Finally, it shall be demonstrated that the proposed method does not only work for $\alpha = 5°$, but also for other intermediate angles of attack, namely $\alpha \in \{1°, 3°, 7°\}$. Table 6 exhibits the lift and drag coefficient computed with CFD and MPE as well as the corresponding relative errors. Note that for all angles of attack the relative error in the lift coefficient is neglectable. The error in the drag coefficient is higher, but with less than one third of a percent more than acceptable.

Table 6. Lift and drag coefficients of the solutions for different angles of attack of the DLR F12 configuration at $M_\infty = 0.2$ computed with MPE using all farfield points and $d = 2$ modes as well as with CFD.

AoA	c_l of MPE (error)	c_l of CFD	c_d of MPE (error)	c_d of CFD
1°	$1.893 \cdot 10^{-1}$ (0.0%)	$1.893 \cdot 10^{-1}$	$8.217 \cdot 10^{-3}$ (0.31%)	$8.192 \cdot 10^{-3}$
3°	$3.869 \cdot 10^{-1}$ (0.03%)	$3.868 \cdot 10^{-1}$	$1.201 \cdot 10^{-2}$ (0.25%)	$1.204 \cdot 10^{-2}$
5°	$5.827 \cdot 10^{-1}$ (0.0%)	$5.827 \cdot 10^{-1}$	$1.983 \cdot 10^{-2}$ (0.15%)	$1.980 \cdot 10^{-2}$
7°	$7.752 \cdot 10^{-1}$ (0.01%)	$7.752 \cdot 10^{-1}$	$3.153 \cdot 10^{-2}$ (0.29%)	$3.144 \cdot 10^{-2}$
9°	$9.631 \cdot 10^{-1}$ (0.05%)	$9.626 \cdot 10^{-1}$	$4.667 \cdot 10^{-2}$ (1.02%)	$4.715 \cdot 10^{-2}$

In addition, a non-intermediate angle of attack, which is outside of the range of the snapshots, is considered. This will be called an extrapolated solution. Although the error is higher, it is with about one percent very good.

Figure 3 visualizes the lift and the drag coefficient which are plotted over the angle of attack. Here, the lines represent the coefficients of the CFD solution, while the asterisks represent those of the MPE solution. All are matched very closely.

Comparison with Thin Plate Spline (TPS) interpolation Next, the results are compared with interpolation [25]. The interpolation is done as follows: The POD coefficients of the snapshots $\boldsymbol{w}_1, \ldots, \boldsymbol{w}_m$ are computed via $a_i(\alpha_j) = (\boldsymbol{u}_i, \boldsymbol{w}_j)_{L_2}$ for $i = 1, \ldots, d$ and $j = 1, \ldots, m$. These coefficients are then interpolated with the help of Thin Plate Spline (TPS) interpolation [26] to obtain suitable POD coefficients $a_i(\alpha^*)$ for the desired angle of attack α^*.

In Table 7 the aerodynamic coefficients as well as their relative errors for two and four modes are given for TPS interpolation. Note that good results are obtained for $\alpha = 3°$ and $\alpha = 5°$, while for the angles close to the boundary of the interpolation range, i.e. $\alpha = 1°$ and $\alpha = 7°$, the error is much higher compared to the MPE error. In fact, MPE approximates solutions better in a global sense. That is, the maximal error of MPE at the considered angles is smaller than the TPS interpolation maximal error.

AoA	c_l of TPS (error)	c_d of TPS (error)
$1°$	$1.891 \cdot 10^{-1}$ (0.11%)	$7.577 \cdot 10^{-3}$ (7.51%)
$3°$	$3.869 \cdot 10^{-1}$ (0.03%)	$1.203 \cdot 10^{-2}$ (0.08%)
$5°$	$5.826 \cdot 10^{-1}$ (0.02%)	$1.985 \cdot 10^{-2}$ (0.25%)
$7°$	$7.748 \cdot 10^{-1}$ (0.06%)	$3.088 \cdot 10^{-2}$ (1.78%)
$9°$	$9.654 \cdot 10^{-1}$ (0.29%)	$5.061 \cdot 10^{-2}$ (7.34%)

Table 7. Lift and drag coefficients of the solutions for different angles of attack of the DLR F12 configuration at $M_\infty = 0.2$ computed with TPS interpolation using $d = 2$ modes.

Also note that the extrapolated solution is much better approximated with MPE compared to interpolation. For TPS interpolation the drag error is with about seven percent unacceptably high.

6 Conclusions

In this work the use of the Missing Point Estimation for reduced order modeling of subsonic steady flows has been considered, where the angle of attack is a system parameter to the reduced order model. The Missing Point Estimation does not solve the equations at each and every point, but at only a selection of points. In this way, independence from the full order is effectively achieved.

The Missing Point Estimation has been tested on the simulation of an inviscid flow past a complex three-dimensional airplane configuration. For this test

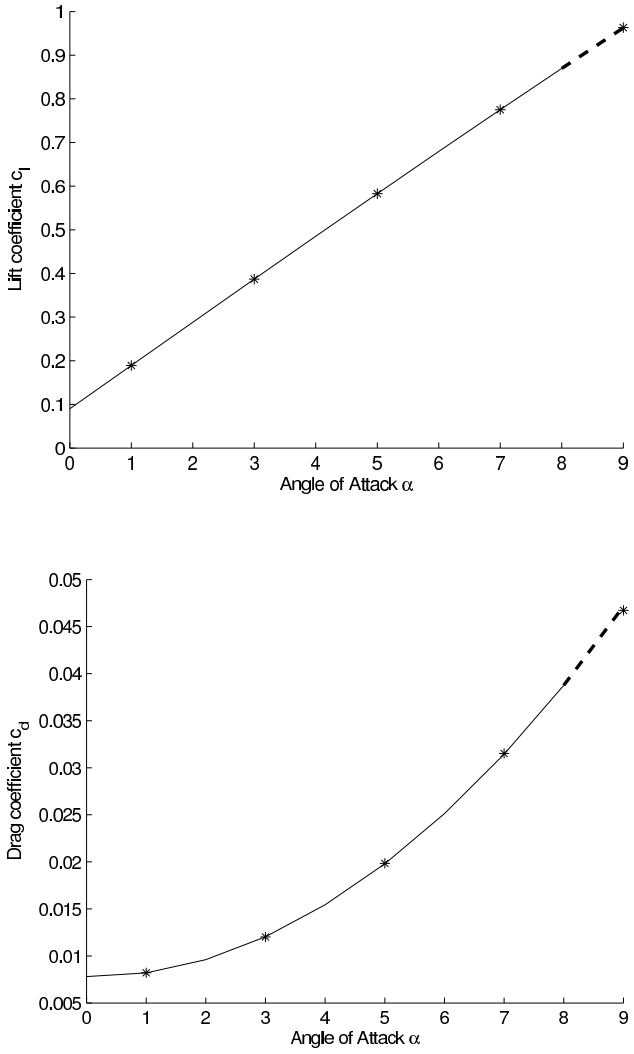

Fig. 3. The aerodynamic coefficients plotted over the angle of attack for the DLR F12 configuration at $M_\infty = 0.2$. The line represents the coefficients of CFD solution and the asterisks represent those of the solution of MPE. Note that the region of extrapolation is indicated by a dashed line. Top: lift coefficient c_l; bottom: drag coefficient c_d.

case it has been shown that, when considering only the farfield points, a good approximation of the aerodynamic coefficient as well as the pressure distribution is obtained. Other point selections do not yield better results and, as a matter of fact, consider more points. Furthermore, the farfield points can easily be identified.

We have seen that for the example considered two basis modes suffice to get an accurate approximation of the flow. Considering more modes actually leads to slightly worse results and the Missing Point Estimation is more unstable with respect to different point selections.

With the proposed method, the solution has been obtained more than a hundred times faster compared to the CFD reference solution. This speed-up is mainly contributed to the fewer residual evaluations needed for the reduced order model.

References

1. European Commission: Flightpath 2050: Europe's Vision for Aviation. Report of the high level group on aviation research, European Union (2011)
2. Klenner, J., Becker, K., Cross, M., Kroll, N.: Future Simulation Concept. In: CEAS Conference Berlin, Session Numerical Simulation. Paper No. 1 (2007)
3. Rossow, C.C., Kroll, N.: Numerical Simulation - Complementing Theory and Experiment as the Third Pillar in Aerodynamics. In Radespiel, R., Rossow, C.C., Brinkmann, B.W., eds.: Hermann Schlichting–100 Years: Scientific Colloquium Celebrating the Anniversary of His Birthday, Braunschweig, Germany 2007. Notes on Numerical Fluid Mechanics and Multidisciplinary Design. Springer (2009)
4. Salas, M.D.: Digital Flight: The Last CFD Aeronautical Grand Challenge. J. Sci. Comput. **28**(2-3) (2006) 479–505
5. Chaturantabut, S., Sorensen, D.C.: Discrete empirical interpolation for nonlinear model reduction. Technical Report TR09-05, CAAM, Rice University (March 2009)
6. Astrid, P., Weiland, S., Willcox, K., Backx, T.: Missing point estimation in models described by proper orthogonal decomposition. IEEE Transactions on Automatic Control **53**(10) (2008) 2237–2251
7. Astrid, P.: Fast reduced order modeling technique for large scale ltv systems. In: Proceedings of the American Control Conference. Volume 1. (July 2004) 762 –767
8. Astrid, P., Verhoeven, A.: Application of Least Squares MPE technique in the reduced order modeling of electrical circuits. In: Proceedings of the 17th Int. Symp. MTNS. (2006) 1980–1986
9. Cardoso, M.A., Durlofsky, L.J., Sarma, P.: Development and application of reduced-order modeling procedures for subsurface flow simulation. International Journal for Numerical Methods in Engineering **77**(9) (2009) 1322–1350
10. Vendl, A., Faßbender, H.: Efficient POD-based Model Order Reduction for steady aerodynamic applications. In Poloni, C., Quagliare, D., Périaux, J., Gauger, N., Giannakoglou, K., eds.: Evolutionary and deterministic methods for design, optimization and control, CIRA, Capua, Italy, EUROGEN 2011 (2011) 296–309
11. Vendl, A., Faßbender, H.: Missing point estimation for steady aerodynamic applications. PAMM **11**(1) (2011) 839–840
12. Lucia, D.J., King, P.I., Beran, P.S.: Reduced order modeling of a two-dimensional flow with moving shocks. Computers & Fluids **32**(7) (2003) 917 – 938

13. Kalashnikova, I., Barone, M.F.: On the stability and convergence of a Galerkin reduced order model (ROM) of compressible flow with solid wall and far-field boundary treatment. International Journal for Numerical Methods in Engineering **83**(10) (2010) 1345–1375
14. Rowley, C., Colonius, T., Murray, R.: Model reduction for compressible flows using POD and Galerkin projection. Physica D: Nonlinear Phenomena **189**(1-2) (2004) 115–129
15. LeGresley, P., Alonso, J.J.: Investigation of non-linear projection for pod based reduced order models for aerodynamics. In: AIAA Paper 2001-0926. 39th AIAA Aerospace Sciences Meeting & Exhibit, Reno, NV (January 8-11 2001)
16. LeGresley, P., Alonso, J.J.: Dynamic domain decomposition and error correction for reduced order models. In: AIAA Paper 2003-0250. 41st AIAA Aerospace Sciences Meeting & Exhibit, Reno, NV (January 6-9 2003)
17. Zimmermann, R.: Towards best-practice guidelines for POD-based reduced order modeling of transonic flows. In Poloni, C., Quagliare, D., Périaux, J., Gauger, N., Giannakoglou, K., eds.: Evolutionary and deterministic methods for design, optimization and control, CIRA, Capua, Italy, EUROGEN 2011 (2011) 326–341
18. Zimmermann, R., Görtz, S.: Non-linear reduced order models for steady aerodynamics. Procedia Computer Science **1** (2010) 165–174
19. Buffoni, M., Telib, H., Iollo, A.: Iterative methods for model reduction by domain decomposition. Computers & Fluids **38**(6) (2009) 1160 – 1167
20. Blazek, J.: Computational Fluid Dynamics: Principles and Applications. first edn. Elsevier (2001)
21. Holmes, P., Lumley, J.L., Berkooz, G.: Turbulence, Coherent Structures, Dynamical Systems and Symmertry. Cambridge, New York (1996)
22. Pinnau, R.: Model reduction via proper orthogonal decomposition. In: Model Order Reduction: Theory, Research Aspects and Applications. Springer (2008) 95–109
23. Powell, M.: A hybrid method for nonlinear equations. Numerical methods for nonlinear algebraic equations **7** (1970) 87–114
24. Gerhold, T., Friedrich, O., Evans, J., Galle, M.: Calculation of complex three-dimensional configurations employing the DLR-TAU-code. AIAA paper **167** (1997)
25. Bui-Thanh, T., Damodaran, M., Willcox, K.: Proper orthogonal decomposition extensions for parametric applications in transonic aerodynamics. AIAA Journal **42**(8) (2004) 1505–1516
26. Forrester, A., Sobester, A., Keane, A.: Engineering Design via Surrogate Modelling: A Practical Guide. Wiley (2008)